Chaparral wildfire shifts the functional potential for soil pyrogenic organic matter and nitrogen cycling

M. Fabiola Pulido-Chavez[1,*], Amelia R. Nelson[2], Michael J Wilkins[2], Sydney I. Glassman[1,*]

[1]Department of Microbiology and Plant Pathology, University of California-Riverside, 900 University Ave, Riverside, CA, 92521
[2]Department of Soil and Crop Sciences, Colorado State University, 307 University Ave, Fort Collins, CO 80521
[3]Department of Environmental Sciences, University of California-Riverside, 900 University Ave, Riverside, CA, 92521
[41]Department of Ecology and Evolutionary Biology, University of California-Irvine

*Corresponding authors: Sydney I Glassman, sydneyg@ucr.edu, and M. Fabiola Pulido-Chavez, fabspulido@gmail.com

Keywords: Pyrophilous bacteria, PyOM, Nitrogen,

Abstract

Wildfires alter soil chemistry and microbial communities, opening niche space for pyrophilous or "fire-loving" microbes to initiate secondary succession. However, wildfires also increase soil nitrogen (N) and transform woody vegetation into difficult-to-degrade pyrogenic organic matter (PyOM), a potential carbon (C) source for pyrophilous microbes. Whether pyrophilous

microbes can degrade these post-fire resources has significant implications for global C and N cycling, including C sequestration and greenhouse gas emissions. To determine temporal patterns in the functional potential for PyOM degradation and N cycling, we performed shotgun metagenomics on 30 burned and unburned soils collected at 17, 25, 34, 131, and 376 days after a high-severity wildfire in a Southern California fire-adapted chaparral shrubland. Not only did overall profiles of C and N cycling genes differ between burned and unburned plots, but burned plots showed dramatic increases from 17 to 376 days in genes responsible for degrading PyOM (167%) and cycling N (117%). In contrast, gene abundances for PyOM degradation and N cycling remained stable over time in unburned plots. Genes encoding the degradation pathways for two PyOM degradation intermediate pathways, catechol and protocatechuate, revealed that the easier-to-degrade ortho-cleavage pathways dominated all time points in the burned plots. Genes encoding N retention pathways (assimilatory and dissimilatory nitrate reduction) dominated N cycling pathways in burned plots for the entire year. Finally, dominant pyrophilous bacterial taxa in the genera *Massilia* and *Noviherbaspirillium* encoded different PyOM and N processing pathways, suggesting that traits enabling adaptation to wildfires, like post-fire resource acquisition, drive microbial secondary succession.

Introduction

Soil microbial communities support fundamental post-fire soil processes such as N immobilization thereby facilitating N storage (1) and C cycling

through decomposition, C sequestration (2) and C loss as CO_2 during respiration (3). However, understanding the complex functional dynamics of the post-fire soil microbiomes remains challenging. With shifting fire regimes resulting in increased fire frequency and severity (4), understanding early changes in the functional potential of post-fire soil microbial communities is necessary to determine how microbes drive secondary successional dynamics and alter important ecosystem functions such as those that affect C sequestration and greenhouse gas (GHG) emissions.

Wildfires often cause reductions in microbial richness, shifting community composition and enabling pyrophilous or “fire-loving” microbes to initiate secondary succession (5-8). Bacterial succession following high-severity wildfires are initiated by the Firmicute and Actinobacteria phyla in various ecosystems including, Southern California Chaparral (8), and redwood-tanoak (5), coniferous (9), and boreal forests (6). At the same time, pyrophilous microbes can trigger a change in resource use that can affect microbial successional dynamics, including successional directionality and community metabolism (10, 11). We previously hypothesized that post-fire microbial succession is initiated by thermotolerators, followed by fast-growing ruderal taxa, who are later supplanted by taxa that capable of capitalizing on post-fire resources, for example bacteria in the genera *Noviherbaspirillium* and *Blastococcu*s (8).This implies that early post-fire taxa might perform metabolic functions that prime the system for colonization by more diverse and complex bacterial species with more specialized metabolic functions, potentially resulting

in a new microbial equilibrium. However, whether these simultaneous functional changes are occurring and subsequently affecting microbial successional dynamics is unknown.

Fires primarily alter the C cycle through the combustion of vegetation (12) and producing abundant PyOM, an aromatic and chemically complex C source known for its resistance to microbial degradation (13, 14). The aromaticity of PyOM requires microbes to encode genes for cleaving aromatic rings thereby metabolizing and acquiring C (15). Bacteria in the genera *Massilia* and *Noviherbaspirillium* are considered putative PyOM degraders (16), and the abundant pyrophilous fungus *Pyronema domesticum* was found to degrade PyOM in laboratory studies (17). Therefore, it is likely that other pyrophilous microbes have the genomic potential to degrade this abundant post-fire C source. However, wildfires can also increase the abundance of short-chain alkanes (18-20), such as propane, which are easier to degrade C sources preferentially selected by microbes for consumption (21-23). However, whether early successional post-fire microbes have the functional potential to degrade PyOM over alkanes or whether C source selection changes with succession is currently unknown.

In addition to altering the C cycle, fires alter the N cycle through N losses via volatilization, reduced urea hydrolysis (24), and a short-term enrichment of bioavailable N (25-27). Indirect wildfire effects, such as removal of the vegetation, can also increase soil NO_3^- and NH_4^+ (27, 28), increase soil temperature, and decrease soil moisture, resulting in increased aerobic conditions

that reduce nitrification (27, 29) and can further impact the microbial community. While microbial immobilization—the uptake of NO_3^- and NH_4^+ for microbial biomass—can decrease denitrification by limiting NO_3^- availability, it can also lead to NO_2 emissions (30, 31). Despite this, denitrification and urea hydrolysis still occur, potentially producing N_2O, a potent greenhouse gas (30-34). Consequently, understanding how pyrophilous microbes treat the increased post-fire bioavailable N has strong implications for GHG emissions. Moreover, post-fire microbial communities likely exhibit varying responses to N depending on the ecosystem type. For example, research in Spanish shrublands three years post-fire, demonstrated increased relative abundances of genes associated with NH_3 assimilation, ammonification, and N_2 fixation (35). In contrast, forested ecosystems in North America showed an increased genomic potential for nitrification and a decrease in denitrification during the first decade after the fire (36). Time since fire also alters the processing of post-fire N, highlighting the complexity of predicting the impact of post-fire microbial succession on N cycling and trace and GHG emissions over time.

We previously sampled a chaparral wildfire at high temporal resolution and showed rapid secondary successional dynamics in the first year post-fire (8). For bacteria, we observed six major compositional turnover events, and we suggest that underlying community metabolic changes might be driving secondary succession (8). Specifically, thermotolerators in the Firmicutes (*Bacillus, Paenibacillus,* and Clostridiales) initially dominated, but were replaced later in the year by taxa with putative N and PyOM degrading

capabilities, including *Massilia* and *Novihersparillum* (8) and potential PyOM degrative capability of *Blastoccocus* (37). From this dataset, we selected a subset of burned and unburned soils from 5 time points (17, 25, 34, 131, and 376 days post-fire) corresponding to high microbial compositional turnover. We conducted a gene-centric metagenomic analysis to determine how temporal changes in pyrophilous communities relate to post-fire bacterial functions and successional dynamics. Specifically, we examined the relative abundance of genes involved in driving PyOM degradation and N cycling over time. We tested the hypotheses that the genes encoding potential for H1) degradation of wildfire-induced C sources like PyOM and alkane and H2) processing of abundant bioavailable N will increase over time in burned plots. We further hypothesized H3) that these changes in gene abundances would correspond with bacterial community shifts and the increased relative abundance of pyrophilous bacteria with the putative abilities to use high post-fire abundances of PyOM and N.

Methods

Sampling

In August-September 2018, the Holy Fire burned 94 km^2 of Manzanita (*Arctostaphylos*) dominated Chaparral shrublands in the Cleveland National Forest in Southern California. Seventeen days post-fire, we established nine plots (6 burned and 3 unburned), selecting for similarity in pre-fire vegetation, elevation, and aspect. Each plot contained four 1 m^2 subplots in each cardinal direction for temporal soil sampling of the top 10 cm of mineral soil beneath the

ash or the duff (Fig. S1). Soil samples were collected at nine time points within the first-year post-fire (17, 25, 34, 67, 95, 131, 187, 286, and 376 days). DNA was extracted from 0.25g of 2mm sieved soil and we performed 16S and ITS2 Illumina MiSeq sequencing of all samples (8). From this data, we selected 5 time points (17, 25, 34, 131, and 376 days post-fire) with extreme bacterial compositional turnover events, and representative burned and unburned plots with high enough quantity and quality DNA for metagenomic sequencing.

Metagenomic sequencing

From each of the 5 timepoints, we selected 3 burned and 3 unburned subplots for a total of 30 metagenomes (15 burned and 15 unburned). Samples were chosen by selecting the DNA samples with the following criteria, 2.5 ng/µl and 230/260 above 1.8, from unburned plot 8 (Fig. S1a) and from two closely situated burned plots with the most similar microbial richness and biomass (plots 2 and 3; Fig. S1a). Metagenomic library preparation and sequencing were performed at the Department of Energy Joint Genome Institute (JGI) in Berkeley, California, for 17 samples and at the University of California, Irvine (UCI) Genomics High-Throughput Facility for 13 samples. Libraries were prepared from the extracted DNA using the Kapa Biosystems library preparation kit at JGI and the Illumina Nextera Flex library preparation kit at UCI and were sequenced on the Illumina NovaSeq 6000 platform on an S4 flow cell (151 bp paired-end reads and a depth of 25 Gb/sample). See supplementary data 1 for additional information regarding metagenomic sequencing.

Metagenomics binning

Sequence adapters were removed from the raw reads using BBduk-v38.89 (sourceforge.net/projects/bbmap/) with the following parameters (ktrim=r, k=23, mink=11, hdist=1). Raw reads were trimmed with Sickle – v1.33 (38) , and the quality of trimmed reads was assessed with FastQC – v0.11.2 (39). Trimmed reads were assembled into contiguous sequences (contigs) with the de novo de Bruijn assembler MEGAHIT – v1.2.9 (40) with the following parameters (min kmer of 27, max of 127, and increment of 10). Per-contig coverage per sample was calculated using CoverM contig version v0.6.0 (41) with the trimmed mean method to retain only mappings >95% identity and minimum alignment of 75% (42). Assembled contigs (>2,500 bp) were binned using MetaBAT2 v2.12.1 with default parameters (43) to assemble metagenome-assembled genomes (MAGs). MAG quality was estimated using checkM v1.1.2 (42) and taxonomy was assigned using GTDB-Tk v2.1.1 (44). To create the final medium and high-quality MAG database, low-quality MAG were removed and the dataset was dereplicated using dRep v3.0.0 (45). See supplementary data 1 for additional information regarding metagenomic assemblies.

Contig annotation

To assess the degradation of aromatic hydrocarbons, such as PyOM, we focused our PyOM contig annotation on catechol and protocatechuate, two intermediate aerobic degradation pathways (46) and short-chain alkane C as the

easier to degrade C source. To improve retention and annotation of the samples in a comprehensive manner, all assembled contigs were annotated using three different databases. First, contigs were annotated using HMMER (47), with hidden Markov models (HMMs) against Kofamscan HMMs (48) to identify specific genes related to aromatic compound degradation (i.e., catechol and protocatechuate and inorganic N cycling) according to previously established methods (11). Second, we used the Calgary approach to AnnoTating HYDrocarbon (CANT-HYD) degradation genes, which uses HMMs for annotating marker genes involved in aerobic and anaerobic hydrocarbon degradation pathways (49). Third, we used the Distilled and Refined Annotation of Metabolism, DRAM (50) annotation tool to profile our contigs through multiple databases (i.e., KEGG (51), UniRef90 (52), MEROPS (53), and Mmseqs2 (54) with the best hits (based on a bit score of 60) reported for each database. The contig dataset was normalized by calculating the contig length corrected trimmed mean (geTMM) of M values (55) using EdgeR (56), normalizing by library depth and gene length as has been previously used for metagenomics data (57-59). The results from all three annotation methods were concatenated into one large file, and genes related to PyOM, alkane degradation, N, and urea cycling were selected for all downstream analyses. In the case where contigs contained duplicated annotations, the annotations were manually curated, and the best functional annotation was determined by selecting the annotation with the lowest e-value.

We used results from a DESeq analysis (see details below) to identify genes of interest, then used NCBI BLAST (60) to link the MAG catalog to these dominant genes. We filtered the BLAST matches to include only hits with 100% identity and a bit score of at least 100. Therefore, we identified the specific taxa that encoded key genes, including those related to PyOM and N cycling pathways. For a comprehensive overview illustrating the bioinformatic procedures employed, please refer to the Fig. S2.

Statistical analysis

All statistical analyses and figures were done in R version 4.2.3 (61). First, we determined how fire, time, and their interaction impacted the overall composition of genes for (H1) PyOM or (H2) N cycling with Permutational Multivariate Analysis of Variance (PERMANOVA;(62)) as implemented in the adonis2 function of the vegan package (63) with 9999 permutations with plot as random effect. Results were visualized using nonmetric multidimensional scaling (NMDS). Ordinations were based on Bray–Curtis distance matrixes using the ordinate function in the phyloseq package (64). Since alkanes increase post-fire and are preferentially selected by microbes as a C source, we separated alkanes from the PyOM genes for all downstream analyses, allowing us to determine if this preferential uptake also occurs in post-fire systems. Moreover, since urease is vital to hydrolyze urea into ammonia (NH_3^+) (65), an essential process that makes N readily available for plant uptake, we further separated the urea pathway from the N cycling processes. Separation of urea from N pathway,

allows us to determine the effect of fire on these important ureases and thus helping us understand if the post-fire microbes possess ureases which can help us better understand post-fire ecosystem restoration and N cycling.

Second, to determine if bacterial functional changes mirrored the rapid compositional changes we previously observed, we plotted the top most abundant bacterial genera in bar plots at 17, 25, 34, 131, and 376 days post-fire (8). We also calculated the homogeneity of variance and used permutest with 9999 permutations and plot as random effect to determine which time points differed for burned and unburned pathways independently. We used principal coordinates analysis (PCoA) to visualize the differences in the homogeneity of variance of each functional pathway with the vegan package using Bray-Curtis dissimilarities.

Third, we independently performed generalized negative binomial regression on burned and unburned plots for each pathway to test how the number of PyOM, alkane, N, and urea cycling genes changed over time. The nestedness level was tested using null model and Akaike criteria. Burned PyOM, alkaline, and urea models included plot, and unburned models included subplot as random effect. Burned N models required plot, subplot, and time, and unburned N models required time and subplot as random effects. For all models, time was scaled and centered. We visualized how the microbial functional potential changes over time by plotting the sum geTMM of each PyOM, alkane, N, and urea pathway using phyloseq version 1.42.0 (64) for each time point in burned and unburned communities independently.

Lastly, to identify the PyOM, alkane, N, and urea genes that were differentially overrepresented in the burned versus the unburned plots at each sampling time point, we employed DESeq2 v1.38.3 (66). Five separate models in DESeq2 were defined, one per timepoint, to assess the response of functional gene potential and independently identify the difference in response to fire over time for each pathway. Results are based on the DESeq Wald test (adjusted p-value < 0.05 and absolute log2 fold-change >0). The total count of differentially abundant genes was visualized as a bar plot for each independent pathway over time. Moreover, we used the differentially abundant genes at each time point in the burned communities (p_{adj}<0.05) to create a metabolic map for PyOM and N degradation pathways. Furthermore, to link the most abundant genes to their taxonomy, we first selected the genes of interest (most abundant genes based on DESeq results at each time point, log2fold change >0 and p < 0.05) and linked them to their respective taxonomy using our MAG dataset using BLAST (Bethesda, 2008). Taxonomy and functional annotation of the selected group of genes were plotted using ggplot2. All statistical scripts (R scripts) are publicly available on GitHub: https://github.com/pulidofabs/Chaparral-Metagenomes.

Results

We assembled 1.2 Tb of metagenomics sequencing data, resulting in the annotation of 2,266,623 genes relevant to post-fire microbial metabolisms. Identified taxa represented across all MAGs belonged to the phyla Acidobacteriota, Proteobacteria, and Verrucomicrobiota *(8).* Additional Of

particular interest, we assembled MAGs of pyrophilous bacteria in the genera *Massilia* and *Noviherbaspirillium*, two of the most dominant genera in our chaparral study(8), contig information, MAG quality and taxonomy information, and contig taxonomy information for the dominant selected genes are available in Supplementary Data 1C.

Wildfire altered the profile of functional genes for PyOM and N

Fire significantly impacted the profile of functional genes associated with N and PyOM cycling, leading to significant changes over time (Fig. 1; Table S1). Wildfire was the strongest driver of differences in functional potential, explaining 15% of the variation for genes affiliated with the processing of PyOM (Fig. 1a) and urea (Fig. 1d) and 16% for alkanes (Fig. 1b), and the remaining N cycling genes (Fig. 1c; Table S1). Time had smaller but significant impacts on the functional profiles of these genes, explaining 5% of the variance in PyOM, N, and urea cycling genes and 6% for alkane genes (Table S1). A significant fire-by-time interaction explained 5% of the variation for PyOM and urea and 6% for N but was not significant for alkanes (Table S1).

While there was no change in the turnover or community-level alterations of the profile of functional genes for PyOM (Fig. 2a), alkane degradation (Fig. 2c), N (Fig. 2e) or urea cycling (Fig. 2g) in the unburned plots (betadisper $p>0.05$), the burned plots experienced multiple functional profile turnover periods for PyOM (Fig. 2b), alkane (Fig. 2d), N (Fig. 2f) and urea cycling genes (Fig. 2h; beta-disper < 0.05; Table S2). Overall, genes associated with urea

processing experienced more turnover events (at 25, 34, and 131 days post-fire) than those associated with the degradation of PyOM, N cycling (34 and 131 days) or alkane degradation (25 and 131 days; Fig. 2).

Time differentially affected PyOM degradation pathways

There was a significant and positive fire by time interaction such that the geTMM normalized gene abundances associated with PyOM or alkane processing increased over time in the burned (Fig. 3b,d), but not unburned plots (Fig. 3a,c; Table S3; S4). This increase is attributed to the increasing number of PyOM genes (Fig. S3), which correlates with increased bacterial diversity and abundance over time (Fig. S4b). Moreover, time differentially affected the different steps of PyOM (Fig. 3b; Table S5) and alkane cycling pathways (Fig. 3d; Table S6) in burned plots such that we detected temporal increases in geTMM values associated with catechol and protocatechuate cycling (Fig. S5; Table S5). However, the β-ketoadipate and all alkane cycling pathways (i.e., alkane and propane pathways) remained unchanged over time (Fig. S5; Table S6).

Time differentially affected N degradation pathways

Similarly, wildfire also had a significant fire by time interaction effect for N and urea such that the geTMM values increased over time in burned (Fig. 4b, d) but not unburned plots (Fig. 4a,c), when compared to 17 days post-fire (Table S3,S4). This increase in geTMM values is due to increased total number of N

cycling genes (Fig. S6), which could be due to increases in bacterial dominance over time (Fig. S4). Moreover, time differentially affected the various steps of the N cycling pathways, resulting in increased geTMM values for NO_3^- assimilation (both assimilatory and dissimilatory) and nitrification in the burned plots compared to 17 days post-fire ($p<0.04$; Fig. 4b; Fig. S7, Table S7). However, denitrification was unaffected by time in the burned plots but did significantly decrease in unburned plots over time (Fig. S7, Table S7). For the urea cycle pathways, both the urea and ornithine geTMM values significantly increased over time in burned plots, whereas there was no effect of time in the unburned plots (Table S8).

Wildfire selects for ortho-cleavage aromatic degradation pathways

Wildfire resulted in a higher number of PyOM degradation genes that were significantly differentially abundant within the burned communities than the unburned communities with particular increases at 131 days post-fire (692 compared to 258; p_{adj} <0.05; Fig. 5a). However, the functional potential for PyOM degradation genes differed across the burned plots over time (p_{adj} <0.05; Fig. 5a, 6). Overall, the ortho-cleavage pathway for the protocatechuate and catechol pathways and the β-ketoadipate pathway were differentially abundant in the burned plots throughout the year (17-131d; p_{adj} <0.05; Fig. 5a, 6). In contrast, the meta-cleavage pathways were only differentially abundant in the early post-fire timepoints, with catechol at 17-25 days and protocatechuate at 17 and 131

days post-fire (p_{adj} <0.05; Fig. 5a, 6). While PyOM degradation genes were detected in the unburned plots at 17-34 days post-fire, it's important to note that these genes are specifically related to lignin degradation (e.g., *ligABCIJKM, galC*; Fig. 5a, 6). Moreover, alkane degradation pathways, propane 2-monooxygenase, alkane hydroxylase, and alkane monooxygenase were only overrepresented in the burned plots at 17d post-fire (p_{adj} <0.05; Fig. 5b).

Wildfire increased genes for N retention

Wildfires resulted in more differentially abundant N cycling genes within the burned communities than the unburned communities (143 compared to 55; Fig. 5c, 7). At all time points, the genes encoding N retention pathways, such as assimilatory NO_3^- (*nasABC, NRT, narK, nrtP*, and *nirA*) and dissimilatory NO_2^- (*nirBD, narBlVHY, and nxrB*) reductase and NO_3^- assimilation (*narG, narZ, nrxA*) pathways were differentially abundant in the burned microbial communities (p_{adj}<0.05; Fig. 5c, 7). In contrast to the unburned plots, where urea cycling pathways were only overrepresented at 17 and 25 days, in the burned plots, all urea degradation pathways were significantly abundant at 25, 34, and 131 days post-fire (p_{adj}<0.05; Fig. 5d,7).

Genomic potential of dominant taxa differed in burned and unburned communities

The genomic potential for catechol and protocatechuate ortho-cleavage and the β-ketoadipate pathway in the burned plots (*fad* genes) were

overrepresented in MAGs representing the phyla Proteobacteria, Actinobacteria, and Acidobacteriota (Fig. 8*;* Supplementary file 1c). Pathway genes for catechol ortho-cleavage (*CatABC)* and β-ketoadipate pathway (*pcaDLJ, fadA)* were differentially encoded by MAG Holy_395.fa, representing the pyrophilous Proteobacteria *Massilia* (Fig. 8), which dominated the 16S sequences in the burned plots across all time points (Fig. S4b). The protocatechuate ortho-cleavage pathway (*pcaBCH*) was encoded by MAGs representing the Burkholderiales-SG8-41 Solirubrobacteraceae (MAG Holy_206.fa) and the pyrophilous bacterial genus *Noviherbaspirillium* (Fig. 8, MAG Holy_399.fa), which dominated at 131 and 376 days post-fire in the burned plots (Fig. S4b). Additionally, genes related to the catechol meta-cleavage pathway (*dmpBC*, *xylEG*) were encoded by the MAGs affiliated with the bacterial families Xanthobacteraceae-PALSA-894 (MAG Holy_369.fa) and Chthoniobacterales-AV80 (*CatE*, MAG Holy_436.fa; Fig. 8). Furthermore, protocatechuate meta-cleavage pathway genes (*ligClK, galC*) were differentially abundant in MAGs representing the dominant *Noviherbaspirillium* (MAG Holy_399.fa) and Xanthobacteraceae-PALSA-894 (MAG Holy_368.fa and Holy_369.fa; Fig. 8). Although catechol, protocatechuate, and β-ketoadipate genomic potential were differentially abundant at 17 and 25 days post-fire in the unburned plots, the genes and the genera differed and were driven by the MAGs representing *Bradyrhizobium* (MAG Holy_362.fa) and Acidimicrobiales-*AC-14* (MAG Holy_71.fa; *pcaD, fadAl; praC, xylH, pracH, ligABC*; Fig. 8).

The genes encoding NO_3^- retention pathways, both assimilatory NO_3^- reductase (*nasABC, nirA*) and dissimilatory NO_3^- reductase (*nirBD*), were differentially abundant in MAGs representing the family Actinobacteriota *Arthrobacter* (*NasABC*; MAG Holy_91.fa), Micromonosporaceae (*NasABC*; *NirBD*; MAG Holy_114.fa) and *Pseudonocardia* (*NirBD*; MAG Holy_153.fa; Fig. 8). The pyrophilous *Massilia* (MAG Holy_395.fa) also encoded genes for N retention, both dissimilatory NO_3^- reductase (*nirD*) and NO_3^- assimilation (*NRT, narK, nrtP, nasA*; Fig. 8). Furthermore, genes associated with NO_3^- assimilation retention pathways (*NRT, narK, nrtP, nasA*) were differentially abundant within the Actinobacteria, specifically in the genus *Arthrobacter* (MAG Holy_91.fa) and family Micromonosporaceae (MAG Holy_114.fa; Fig. 8). Like PyOM genes, NO_3^- assimilation retention pathways , reduction, and denitrification in the unburned plots at 17 days post-fire were differentially abundant in the non-pyrophilous bacterial genus *Bradyrhizobium* (MAG Holy_362.fa and Holy_361.fa; *NRT, narK, nrtP, nasAC, napA*; Fig. 8).

Discussion

We found that high-severity fire dramatically altered the genomic functional potential of the post-fire soil microbiome, concurrent with large changes in the bacterial community composition (Pulido-Chavez et al., 2023). Wildfire increased the geTMM of PyOM degradation genes in burned plots over time, and our analyses revealed that catechol and protocatechuate ortho-cleavage (i.e., β-ketoadipate) pathways are the preferred pathway for PyOM degradation.

We also found that wildfire increased the geTMM values for N cycling genes in burned plots over time, selecting for genes encoding the N retention pathways, via conversion of NO_3^- to biomass and NO_2 to NH_3^+, with significant implications for trace and GHG emissions. Finally, we found that pyrophilous bacterial taxa that dominated our post-fire chaparral communities (i.e., Burkholderiales, *Massilia,* and *Noviherbaspirillium*) (Pulido-Chavez et al., 2023) encoded multiple but different PyOM degradation and N cycling pathways, suggesting that traits enabling adaptation to wildfires like post-fire resource acquisition drive microbial succession.

PyOM geTMM values increased over time in burned plots

We previously observed patterns of secondary succession in chaparral and hypothesized that these changes aligned with the ability of post-fire microbes to use post-fire resources (8). Here, we found that the normalized abundance of genes encoding for PyOM degradation increased over time and were differentially abundant in the burned plots. Given the previously observed increases in bacterial species richness and diversity over time ((8), Fig. S4), and the concurrent increase in total number of differentially abundant genes in this study, it is plausible that the elevated geTMM is associated with the emergence of additional bacterial species encoding functional potential for PyOM degradation.

We hypothesized that the succession of post-fire microbes is such that thermotolerant microbes dominate first, followed by fast-colonizers, which are

then replaced by microbes capable of capitalizing on post-fire resources, such as PyOM and N (8). Our results support those inferences and indicate that MAGs representing pyrophilous bacteria Proteobacteria *Noviherbaspirillum* and *Massilia*, which dominate in the first year post-fire, encode multiple genes for PyOM and N degradation particularly at 131 days post-fire (Fig. 6). Indeed, studies involving PyOM treatments (67-69) and incubation studies (70, 71) have demonstrated an increase in the relative abundance of *Noviherbaspirillum* and *Massilia*, indicating their active degradation of PyOM as a C source. In our study (5), *Noviherbaspirillium* increased in abundance over time and dominated at 131 and 376 days post-fire, whereas *Massilia* dominated at all post-fire time points but was particularly dominant at 34 and 131 days post-fire.

Here, we showed that *Massilia* encoded genes for PyOM degradation via the catechol and β-ketoadipate ortho-cleavage pathway while *Noviherbaspirillium* favored the protocatechuate ortho and meta-cleavage pathways for PyOM degradation. The difference in their degradation pathways may explain the delayed appearance of *Noviherbaspirillum* during succession, as microbes using the meta-cleavage pathway often experience a growth lag and delayed substrate utilization due to regulatory difficulties in inducing degradation of intermediate PyOM pathways (72). In contrast, the dominance of *Massilia* could be attributed to its genomic potential for rapid access to C via the catechol ortho-cleavage pathway.

While we had previously shown successional patterns for post-fire fungal communities ((5), Fig. S4), metagenomic analysis for fungi lags behind that of

bacteria, so no fungal-associated MAGs were detected in our data. However, current research using whole transcriptome sequencing revealed that *Aspergillus*, a dominant fungus across all of our post-fire timepoints (8), possesses some genes involved in the β-ketoadipate pathway (73). Thus, it is possible that the temporal increase in PyOM cycling genes observed in our study is partly due to an increase in fungal diversity over time. However, further analyses are required to better develop this hypothesis.

Fire also selects for microbial taxa that encode genes for alkane degradation. Previous studies have shown that extractable levels of acetate increase post-fire in subsurface soil (74). In this study, we demonstrate that bacteria in the early post-fire stages, specifically at 17 and 25 days post-fire, possess the genomic capacity to use this abundant post-fire resource, as indicated by the higher abundance of genes such as *ACSS1_2*, *acs*, and *pta* associated with the activation of acetate for use in central metabolism. This suggests that early post-fire bacteria might prefer to degrade labile C sources that support rapid growth, enabling these populations to dominate the ecosystem. However, later in the succession process, the potential depletion of labile C sources leads to community shifts, with microbes capable of using more complex aromatic C sources rapidly dominating the community. Together, these findings highlight the intricate interactions that may occur post-fire and suggest that metabolic handoffs and cooperative resource use may play crucial roles in shaping post-fire successional and ecosystem dynamics.

Post-fire microbes preferentially retain N and increase nitrification

Soil N cycling, primarily mediated by microbes, is crucial in the post-fire environment and has strong implications for trace and GHG emissions (25). Coinciding with significant increases in bioavailable N after the fire, our study revealed that geTMM values for genes encoding nitrification, assimilatory, and dissimilatory N reductase increased over time and exhibited differential abundance in the burned plots. These results are supported by complementary post-fire studies in coniferous forests (36, 75-78) and chaparral (79) ecosystems indicating enrichment of nitrification in the immediate aftermath of wildfire. Our previous research indicated an increase in *Massilia* and *Paenibacillus* over time following the fire (8), and previous research shows *Paenibacillus* can fix nitrogen (80, 81) supporting the observed increase in genes related to nitrification, assimilatory, and dissimilatory N reductase in our study. Additionally, N immobilization peaked after 131 days, coinciding with increased abundance of *Arthrobacter* and *Micromonosporaceae*, both of which were found to encode genes for N immobilization. Thus, our research suggests that during succession, simultaneous functional changes are occurring and subsequently driving bacterial successional dynamics, whereby a few bacterial taxa with more specialized metabolic functions dominate and control bacterial successional dynamics.

Wildfire-induced short-term N losses via increased microbial retention of NO_3^- can be detrimental to post-fire ecosystem recovery (79), especially when microbes, the major players in N retention (79, 82), are also affected by the fire.

Our study revealed an overrepresentation of denitrification genes (*nirK*, *narG*, *narZ*, *nxrA*) in early post-fire pyrophilous bacteria (17-25 days post-fire), which may exacerbate N losses in the form of N_2O, potent greenhouse gases. These findings are consistent with a review of wildfire-affected ecosystems (83). However, N losses are transient, as post-fire microbes, including those associated with the genera *Arthrobacter*, *Massilia*, *Blastocatellia*, and the family Micromonosporaceae, have the capacity to immobilize N through the assimilatory NO_3- reduction pathway, incorporating it into biomass. Moreover, the genera *Massilia*, *Pseudonocardia*, and *Micromonosporaceae* can further convert NO_2^- to NH_3^+ via dissimilatory NO_2^- reductase (*nirBD*), making this resource readily available for plant and microbial use. These results demonstrate that post-fire microbes possess the genomic potential to retain N in the ecosystem. Previous observations of N retention processes, such as microbial N immobilization, have been documented in various wildfire-affected systems (84), including chaparral (85), and in field studies involving PyOM additions (86). In this study, we observed an increase in the abundance of genes related to N incorporation by MAGs representing pyrophilous genera *Massilia* and *Arthrobacter* consistent with prior research highlighting the N-reducing and assimilating capabilities of both *Massilia* and *Arthrobacter* (87-90). Furthermore, metagenomic studies have previously shown enrichment of *nirB/D* genes (N retention genes) four years post-fire (36). These collective results underscore the role that dominant pyrophilous bacteria in fire-adapted chaparral communities

may play in the assimilation and retention of ecosystem N, playing critical roles in mitigating N losses and facilitating ecosystem restoration.

Post-fire chaparral microbes preferentially degrade PyOM via the ortho-cleavage degradation pathway

Microbial taxa enriched in the post-fire soils encoded the ortho-cleavage catechol and protocatechuate pathways for PyOM degradation more so than the meta-cleavage pathways. However, the bacterial taxa implicated in PyOM degradation only contained functional genes for part of a specific degradation pathway, suggesting that post-fire bacterial communities may thrive via cooperative interactions and metabolic handoffs. Prior studies have shown that the β-ketoadipate pathway (e.g., ortho-cleavage pathway) is the most common method for aromatic degradation and the dominant route for aromatic degradation for lignin-degrading bacteria (91, 92). These results are also supported by data from post-fire coniferous forest soils, which revealed the presence of the ortho-cleavage pathway in over 50% of MAGs (11) and intriguingly suggests that high-severity fires may select for ortho-cleavage pathways regardless of the biome. Furthermore, we found that the genes for the full catechol (*catABC*) and protocatechuate (*pcaHGBCDLJ*) ortho-cleavage degradation pathways were present across all the burned plots for the entire year. The differentially abundant ortho-cleavage pathway genes were linked to MAGs representing multiple taxa in the Proteobacteria phylum, including *Noviherbaspirillum* (Holy_399.fa and Holy_399.fa), *Massilia* (Holy_395.fa), and

Xanthobacteraceae PALSA-89 (Holy_368.fa and Holy_369.fa), the Acidobacteriota phylum, Chthoniobacterales AV80 (Holy_436.fa) and the Actinobacteriota phylum, *Pseudonocardia* (Holy_153.fa), and Solirubrobacteraceae (Holy_206.fa). Previous research indicated that bacteria preferentially use the catechol ortho-cleavage pathway while fungi preferentially use the protocatechuate ortho-cleave pathway (46), suggesting that there is interspecies competition for the same resource pool between pyrophilous bacteria and fungi.

The catechol and protocatechuate orthocleavage pathways are biochemically conserved with high diversity in the level of gene organization (93, 94), which may indicate that pyrophilous microbes from wildfire-adapted ecosystems such as chaparral have evolved mechanisms to capitalize on PyOM as a C source. This is corroborated by the high relative abundance of differentially abundant PyOM degradation genes in our burned plots. Our findings indeed revealed differentially abundant PyOM genes, which were linked to MAGs representing the Actinomycetales *Arthrobacter* (Holy_91.fa), *Pseudonocardia* (Holy_153.fa), Micromonosporaceae (Holy_114.fa), as well as *Noviherbaspirillum* (Holy_399.fa and Holy_399.fa), and *Massilia* (Holy_395.fa and Holy_395.fa). Previous research shows that *Arthrobacter* (11) and Burkholderiales encode genes for aromatic compound catabolism (95), supporting our results. The ortho-cleavage pathway provides a growth advantage to microbes (96) by efficiently converting C to cell mass (97-99) and both pyrophilous *Massilia* and *Noviherbaspirillum* are fast-growing bacteria (100,

101) that dominated this system (8) and contained genes for PyOM degradation. Together, these results suggest that in a post-fire system, where C is in the form of commonly considered recalcitrant PyOM, pyrophilous bacteria prefer the easier-to-degrade PyOM processing pathway (ortho-cleavage pathway), rapidly converting PyOM to biomass and thus dominating and initiating microbial succession, as previously suggested (8).

Conclusions

Our high-resolution gene-centric metagenomic analysis allowed us to detect the rapid enrichment of genomic functional potential for the processing of PyOM, inorganic N, alkanes, and urea in burned plots during the first post-fire year, coinciding with the dominance of pyrophilous bacteria in the post-fire soils. We found that MAGs representing the putative pyrophilous *Massilia* and *Noviherbaspirillium* preferentially encode the ortho-cleavage catechol and protocatechuate degradation pathways while assimilating N to acquire energy, potentially minimizing GHG emissions. Interestingly, post-fire bacteria employed distinct pathways for the degradation of post-fire resources such as PyOM and N, suggesting that metabolic handoffs are common within post-fire bacterial communities. This indicates that traits which have evolved for survival after fires, especially those associated with acquiring resources, are the primary drivers of bacterial secondary successional dynamics. While the capability of post-fire bacteria to capitalize on PyOM and N has been previously hypothesized (8, 71), and shown for some taxa (11, 17, 35), our research unveils previously

unknown functional changes over a high resolution successional timeline, filling a critical gap created by limited post-fire sampling efforts**.** Thus, our work significantly contributes to our understanding of post-wildfire bacterial ecology and provides valuable insights into the intricate dynamics of bacterial communities in fire-affected ecosystems.

3.7 Acknowledgments

We thank the Joint Genome Institute (JGI) Community Sequencing Project (CSP) New Investigator Award 507364 to SIG, the Bureau of Land Management (BLM) Joint Fire Science Program (JFSP) Graduate Research Innovation (GRIN) Award 012641□002 to MFPC and SIG, the United States Department of Agriculture (USDA)-NIFA Award #2022-67014-36675 to SIG, and the Department of Energy (DOE) BER Award #DE-SC0023127 to SIG and MJW for funding this project. We further thank the Cleveland National Forest and the Trabuco Ranger District, including District Ranger Darrel Vance and Emily Fudge, Jeffrey Heys, Lauren Quon, Jacob Rodriguez, and Victoria Stempniewicz, for their help with permitting. We thank JGI Metagenome Program, including Nicole Shapiro, Natasha Brown, Emiley Eloe-Fadrosh, and Simon Roux, for their help in processing and submitting our metagenomic samples. Lastly, we thank Judy A. Chung, Aral C. Greene, Elizah Stephens, Dylan Enright, and Sameer S. Saroa for fieldwork assistance and James Randolph for molecular assistance. We thank Jason Stajich and Pete Homyak and our anonymous reviewers for helpful feedback on the manuscript.

3.8 Competing Interests

The authors declare no competing or conflicts of interest.

3.9 Data Availability Statement

The metagenomic reads and bacterial MAGs have been deposited to the National Center for Biotechnology Information Sequence Read Archive under BioProject PRJNA761539. Amplicon sequence reads for bacterial 16S rRNA and fungal ITS2 have been deposited to the National Center for Biotechnology Information Sequence Read Archive under BioProject PRJNA761539. All statistical R scripts/codes are available on GitHub

and include the sample metadata required for analysis https://github.com/pulidofabs/Chaparral-Metagenomes.

3.10 References

1. Turner MG, Smithwick EAH, Metzger KL, Tinker DB, Romme WH. Inorganic nitrogen availability after severe stand-replacing fire in the Greater Yellowstone ecosystem. Proceedings of the National Academy of Sciences. 2007;104(12):4782–9.
2. Raza T, Qadir MF, Khan KS, Eash NS, Yousuf M, Chatterjee S, et al. Unrevealing the potential of microbes in decomposition of organic matter and release of carbon in the ecosystem. Journal of Environmental Management. 2023;344:118529.
3. Liu W, Zhang Z, Li J, Wen Y, Liu F, Zhang W, et al. Effects of fire on the soil microbial metabolic quotient: A global meta-analysis. CATENA. 2023;224:106957.
4. Riley KL, Loehman RA. Mid-21st-century climate changes increase predicted fire occurrence and fire season length, Northern Rocky Mountains, United States. Ecosphere. 2016;7(11):e01543.
5. Enright DJ, Frangioso KM, Isobe K, Rizzo DM, Glassman SI. Mega-fire in Redwood Tanoak Forest Reduces Bacterial and Fungal Richness and Selects for Pyrophilous Taxa that are Phylogenetically Conserved. Molecular Ecology. 2022;31:2475–93.
6. Whitman T, Whitman E, Woolet J, Flannigan MD, Thompson DK, Parisien M-A. Soil bacterial and fungal response to wildfires in the Canadian boreal forest across a burn severity gradient. Soil Biology and Biochemistry. 2019;138:107571.
7. Fox S, Sikes BA, Brown SP, Cripps CL, Glassman SI, Hughes K, et al. Fire as a driver of fungal diversity — A synthesis of current knowledge. Mycologia. 2022;114(2):1-27.
8. Pulido-Chavez MF, Randolph JWJ, Zalman C, Larios L, Homyak PM, Glassman SI. Rapid bacterial and fungal successional dynamics in first year after chaparral wildfire. Molecular Ecology. 2023;32(7):1685-707.
9. Caiafa MV, Nelson AR, Borch T, Roth HK, Fegel TS, Rhoades CC, et al. Distinct fungal and bacterial responses to fire severity and soil depth across a ten-year wildfire chronosequence in beetle-killed lodgepole pine forests. Forest Ecology and Management. 2023;544:121160.
10. Luo Y, Huang Y, Xu R-x, Qian B, Zhou J-w, Xia X-l. Primary and Secondary Succession Mediate the Accumulation of Biogenic Amines during Industrial Semidry Chinese Rice Wine Fermentation. Applied and Environmental Microbiology. 2020;86(17):e01177-20.

11. Nelson AR, Narrowe AB, Rhoades CC, Fegel TS, Daly RA, Roth HK, et al. Wildfire-dependent changes in soil microbiome diversity and function. Nat Microbiol. 2022;7(9):1419-30.
12. Nave L, Vance. E, . CS, Curtis. P. Fire effects on temperate forest soil C and N storage. Ecol Appl. 2011;4:1189-201.
13. Knicker H. Pyrogenic organic matter in soil: Its origin and occurrence, its chemistry and survival in soil environments. Quaternary International. 2011;243(2):251-63.
14. Bird MI, Wynn JG, Saiz G, Wurster CM, McBeath A. The Pyrogenic Carbon Cycle. Annual Review of Earth and Planetary Sciences. 2015;43(1):273-98.
15. Haddock JD. Aerobic Degradation of Aromatic Hydrocarbons: Enzyme Structures and Catalytic Mechanisms. Handbook of Hydrocarbon and Lipid Microbiology2010. p. 1057-69.
16. Perez-Pantoja D, Donoso R, Agullo L, Cordova M, Seeger M, Pieper DH, et al. Genomic analysis of the potential for aromatic compounds biodegradation in Burkholderiales. Environ Microbiol. 2012;14(5):1091-117.
17. Fischer MS, Stark FG, Berry TD, Zeba N, Whitman T, Traxler MF. Pyrolyzed Substrates Induce Aromatic Compound Metabolism in the Post-fire Fungus, Pyronema domesticum. Front Microbiol. 2021;12:729289.
18. Badía D, Martí C, Aguirre AJ, Aznar JM, González-Pérez JA, De la Rosa JM, et al. Wildfire effects on nutrients and organic carbon of a Rendzic Phaeozem in NE Spain: Changes at cm-scale topsoil. CATENA. 2014;113:267-75.
19. González-Pérez JA, González-Vila FJ, Almendros G, Knicker H. The effect of fire on soil organic matter—a review. Environment International. 2004;30(6):855-70.
20. Kuhn TK, Krull ES, Bowater A, Grice K, Gleixner G. The occurrence of short chain n-alkanes with an even over odd predominance in higher plants and soils. Organic Geochemistry. 2010;41(2):88-95.
21. Abbasian F, Lockington R, Mallavarapu M, Naidu R. A Comprehensive Review of Aliphatic Hydrocarbon Biodegradation by Bacteria. Appl Biochem Biotechnol. 2015;176(3):670-99.
22. Moucawi J, Fustec E, Jambu P, Amblfs A, Jacquesy R. Biooxidation of added and natural hydrocarbons in soils: Effect of iron. Soil Biology and Biochemistry. 1981;13(5):335-42.
23. Thomas CL, Jansen B, van Loon EE, Wiesenberg GLB. Transformation of *n*-alkanes from plant to soil: a review. SOIL. 2021;7(2):785-809.
24. Goberna M, Garcia C, Insam H, Hernandez MT, Verdu M. Burning fire-prone Mediterranean shrublands: immediate changes in soil microbial community structure and ecosystem functions. Microb Ecol. 2012;64(1):242-55.
25. Dannenmann M, Díaz-Pinés E, Kitzler B, Karhu K, Tejedor J, Ambus P, et al. Postfire nitrogen balance of Mediterranean shrublands: Direct

combustion losses versus gaseous and leaching losses from the postfire soil mineral nitrogen flush. Global Change Biology. 2018;24(10):4505-20.

26. Johnson DW, Curtis PS. Effects of forest management on soil C and N storage: meta analysis. Forest Ecology and Management. 2001;140(2-3):227-38.
27. Neary DG, Klopatek CC, DeBano LF, Ffolliott PF. Fire effects on belowground sustainability: a review and synthesis. Forest Ecology and Management. 1999;122(1-2):51-71.
28. DeBano LF, Neary DG, Ffolliott PF. Fire Effects on Ecosystems. 1998.
29. Ayiti OE, Babalola OO. Factors Influencing Soil Nitrification Process and the Effect on Environment and Health. Frontiers in Sustainable Food Systems. 2022;6.
30. Chen H, Ma K, Huang Y, Yao Z, Chu C. Stable Soil Microbial Functional Structure Responding to Biodiversity Loss Based on Metagenomic Evidences. Frontiers in Microbiology. 2021;12.
31. Hoang HG, Thuy BTP, Lin C, Vo D-VN, Tran HT, Bahari MB, et al. The nitrogen cycle and mitigation strategies for nitrogen loss during organic waste composting: A review. Chemosphere. 2022;300:134514.
32. Singh J, Kunhikrishnan A, Bolan NS, Saggar S. Impact of urease inhibitor on ammonia and nitrous oxide emissions from temperate pasture soil cores receiving urea fertilizer and cattle urine. The Science of the Total Environment. 2013;465:56-63.
33. Yoon S, Song B, Phillips RL, Chang J, Song MJ. Ecological and physiological implications of nitrogen oxide reduction pathways on greenhouse gas emissions in agroecosystems. FEMS Microbiology Ecology. 2019;95(6):fiz066.
34. Thomson AJ, Giannopoulos G, Pretty J, Baggs EM, Richardson DJ. Biological sources and sinks of nitrous oxide and strategies to mitigate emissions. Philosophical Transactions of the Royal Society B: Biological Sciences. 2012;367(1593):1157-68.
35. Cobo-Díaz JF, Fernández-González AJ, Villadas PJ, Robles AB, Toro N, Fernández-López M. Metagenomic Assessment of the Potential Microbial Nitrogen Pathways in the Rhizosphere of a Mediterranean Forest After a Wildfire. Microbial Ecology. 2015;69(4):895-904.
36. Dove NC, Tas N, Hart SC. Ecological and genomic responses of soil microbiomes to high-severity wildfire: linking community assembly to functional potential. ISME J. 2022;16(7):1853-63.
37. Guo M, Shang X, Ma Y, Zhang K, Zhang L, Zhou Y, et al. Biochars assisted phytoremediation of polycyclic aromatic hydrocarbons contaminated agricultural soil: Dynamic responses of functional genes and microbial community. Environmental Pollution. 2024;345.
38. Joshi NA FJ. Sickle: A sliding-window, adaptive, quality-based trimming tool for FastQ files 2011;Version 1.33.

39. Andrews S. FastQC: A Quality Control Tool for High Throughput Sequence Data [Online]. 2010.

40. Li D, Liu C-M, Luo R, Sadakane K, Lam T-W. MEGAHIT: An ultra-fast single-node solution for large and complex metagenomics assembly via succinct de Bruijn graph. arXiv:14097208 [q-bio]. 2014.
41. Woodcroft BJ. CoverM. Queensland University of Technology Centre for Microbiome Research: School of Biomedical Sciences; 2007.
42. Parks DH, Imelfort M, Skennerton CT, Hugenholtz P, Tyson GW. CheckM: assessing the quality of microbial genomes recovered from isolates, single cells, and metagenomes. Genome Res. 2015;25(7):1043-55.
43. Kang DD, Froula J, Egan R, Wang Z. MetaBAT, an efficient tool for accurately reconstructing single genomes from complex microbial communities. PeerJ. 2015;3:e1165.
44. Chaumeil P-A, Mussig AJ, Hugenholtz P, Parks DH. GTDB-Tk: a toolkit to classify genomes with the Genome Taxonomy Database. Bioinformatics. 2019:btz848.
45. Olm MR, Brown CT, Brooks B, Banfield JF. dRep: a tool for fast and accurate genomic comparisons that enables improved genome recovery from metagenomes through de-replication. The ISME Journal. 2017;11(12):2864-8.
46. Fuchs G, Boll M, Heider J. Microbial degradation of aromatic compounds - from one strategy to four. Nat Rev Microbiol. 2011;9(11):803-16.
47. Eddy SR. Accelerated Profile HMM Searches. PLOS Computational Biology. 2011;7(10):e1002195.
48. Aramaki T, Blanc-Mathieu R, Endo H, Ohkubo K, Kanehisa M, Goto S, et al. KofamKOALA: KEGG Ortholog assignment based on profile HMM and adaptive score threshold. Bioinformatics. 2020;36(7):2251-2.
49. Khot V, Zorz J, Gittins DA, Chakraborty A, Bell E, Bautista MA, et al. CANT-HYD: A Curated Database of Phylogeny-Derived Hidden Markov Models for Annotation of Marker Genes Involved in Hydrocarbon Degradation. Frontiers in Microbiology. 2022;12.
50. Shaffer M, Borton MA, McGivern BB, Zayed AA, Rosa SLL, Solden LM, et al. DRAM for distilling microbial metabolism to automate the curation of microbiome function. bioRxiv. 2020:2020.06.29.177501.
51. Kanehisa M, Goto S. KEGG: Kyoto Encyclopedia of Genes and Genomes. Nucleic Acids Research. 2000;28(1):27-30.
52. Suzek BE, Huang H, McGarvey P, Mazumder R, Wu CH. UniRef: comprehensive and non-redundant UniProt reference clusters. Bioinformatics. 2007;23(10):1282-8.
53. Rawlings ND, Waller M, Barrett AJ, Bateman A. *MEROPS* : the database of proteolytic enzymes, their substrates and inhibitors. Nucleic Acids Research. 2014;42(D1):D503-D9.
54. Steinegger M, Söding J. MMseqs2 enables sensitive protein sequence searching for the analysis of massive data sets. Nat Biotechnol. 2017;35(11):1026-8.
55. Smid M, Coebergh van den Braak RRJ, van de Werken HJG, van Riet J, van Galen A, de Weerd V, et al. Gene length corrected trimmed mean of M-values (GeTMM) processing of RNA-seq data performs similarly in

intersample analyses while improving intrasample comparisons. BMC Bioinformatics. 2018;19(1):236.

56. Robinson MD, McCarthy DJ, Smyth GK. edgeR: a Bioconductor package for differential expression analysis of digital gene expression data. Bioinformatics (Oxford, England). 2010;26(1):139-40.

57. Capo E, Broman E, Bonaglia S, Bravo AG, Bertilsson S, Soerensen AL, et al. Oxygen deficient water zones in the Baltic Sea promote uncharacterized Hg methylating microorganisms in underlying sediments. Limnology and Oceanography. 2021;67(1):135-46.

58. Leleiwi I, Rodriguez-Ramos J, Shaffer M, Sabag-Daigle A, Kokkinias K, Flynn RM, et al. Exposing new taxonomic variation with inflammation - a murine model-specific genome database for gut microbiome researchers. Microbiome. 2023;11(1):114.

59. Santos-Medellin C, Blazewicz SJ, Pett-Ridge J, Firestone MK, Emerson JB. Viral but not bacterial community successional patterns reflect extreme turnover shortly after rewetting dry soils. Nat Ecol Evol. 2023;7(11):1809-22.

60. Bethesda. Building a BLAST database with your (local) sequences:BLAST Command Line Applications User Manual. National Center for Biotechnology Information. 2008.

61. RCoreTeam. R: A language and environment for statistical computing. R Foundation for Statistical Computing. Vienna, Austria.2023.

62. Anderson MJ. Permutational Multivariate Analysis of Variance (PERMANOVA). Wiley StatsRef: Statistics Reference Online: John Wiley & Sons, Ltd; 2017. p. 1-15.

63. Oksanen J, Simpson G, Blanchet F, Kindt R, Legendre P, Minchin P, et al. vegan: Community Ecology Package. 2022.

64. McMurdie PJ, Holmes S. Phyloseq: An R Package for Reproducible Interactive Analysis and Graphics of Microbiome Census Data. . PLOS ONE. 2013;8(4):e61217.

65. Fernández-García V, Marcos E, Reyes O, Calvo L. Do Fire Regime Attributes Affect Soil Biochemical Properties in the Same Way under Different Environmental Conditions? Forests. 2020;11(3):274.

66. Love MI, Huber W, Anders S. Moderated estimation of fold change and dispersion for RNA-seq data with DESeq2. Genome Biol. 2014;15(12):550.

67. Chen Z, Tu X, Meng H, Chen C, Chen Y, Elrys AS, et al. Microbial process-oriented understanding of stimulation of soil N2O emission following the input of organic materials. Environmental Pollution. 2021;284:117176.

68. Zeba N, Berry TD, Fischer MS, Traxler MF, Whitman T. Soil carbon mineralization and microbial community dynamics in response to PyOM addition. preprint. Ecology; 2023 2023/06/22/.

69. Cheng H, Tang G, Wang S, Rinklebe J, Zhu T, Cheng L, et al. Combined remediation effects of biochar and organic fertilizer on immobilization and dissipation of neonicotinoids in soils. Environ Int. 2022;169:107500.

70. Song H-K, Song W, Kim M, Tripathi BM, Kim H, Jablonski P, et al. Bacterial strategies along nutrient and time gradients, revealed by metagenomic analysis of laboratory microcosms. FEMS Microbiology Ecology. 2017;93(fix114).
71. Woolet J, Whitman T. Pyrogenic organic matter effects on soil bacterial community composition. Soil Biology and Biochemistry. 2020;141:107678.
72. Johnson CW, Beckham GT. Aromatic catabolic pathway selection for optimal production of pyruvate and lactate from lignin. Metabolic Engineering. 2015;28:240-7.
73. Sgro M, Chow N, Olyaei F, Arentshorst M, Geoffrion N, Ram AFJ, et al. Functional analysis of the protocatechuate branch of the β-ketoadipate pathway in Aspergillus niger. Journal of Biological Chemistry. 2023;299(8):105003.
74. Blank RR, Allen F, Young JA. Extractable Anions in Soils following Wildfire in a Sagebrush-Grass Community. Soil Science Society of America Journal. 1994;58(2):564-70.
75. Dove NC, Klingeman DM, Carrell AA, Cregger MA, Schadt CW. Fire alters plant microbiome assembly patterns: integrating the plant and soil microbial response to disturbance. New Phytologist. 2021;230(6):2433-46.
76. Kurth VJ, Fransioli N, Perez FZ, Hart SC, Gehring CA. Stand-replacing wildfires alter the community structure of wood-inhabiting fungi in southwestern ponderosa pine forests of the USA | Elsevier Enhanced Reader. 2013.
77. Dove NC, Safford HD, Bohlman GN, Estes BL, Hart SC. High-severity wildfire leads to multi-decadal impacts on soil biogeochemistry in mixed-conifer forests. Ecol Appl. 2020;30(4):e02072.
78. Kurth VJ, Hart SC, Ross CS, Kaye JP, Fule PZ. Stand-replacing wildfires increase nitrification for decades in southwestern ponderosa pine forests. Oecologia. 2014;175(1):395-407.
79. Hanan EJ, Tague C, Schimel JP. Nitrogen cycling and export in California chaparral: the role of climate in shaping ecosystem responses to fire. Ecological Monographs. 2016;87(1):76-90.
80. Monciardini P, Cavaletti L, Schumann P, Rohde M, Donadio S. Conexibacter woesei gen. nov., sp. nov., a novel representative of a deep evolutionary line of descent within the class Actinobacteria. Int J Syst Evol Microbiol. 2003;53(Pt 2):569-76.
81. Slepecky RA, Hemphill HE. The Genus Bacillus—Nonmedical. In: Dworkin M, Falkow S, Rosenberg E, Schleifer K-H, Stackebrandt E, editors. The Prokaryotes: Volume 4: Bacteria: Firmicutes, Cyanobacteria. New York, NY: Springer US; 2006. p. 530-62.
82. Knicker H. How does fire affect the nature and stability of soil organic nitrogen and carbon? A review. Biogeochemistry. 2007;85(1):91-118.
83. Stephens EZ, Homyak PM. Post-fire soil emissions of nitric oxide (NO) and nitrous oxide (N2O) across global ecosystems: a review. Biogeochemistry. 2023.

84. Xu W, Elberling B, Ambus PL. Fire increases soil nitrogen retention and alters nitrogen uptake patterns among dominant shrub species in an Arctic dry heath tundra. Sci Total Environ. 2022;807(Pt 3):150990.
85. Goodridge BM, Hanan EJ, Aguilera R, Wetherley EB, Chen Y-J, D'Antonio CM, et al. Retention of Nitrogen Following Wildfire in a Chaparral Ecosystem. Ecosystems. 2018;21(8):1608-22.
86. Bai SH, Reverchon F, Xu C-Y, Xu Z, Blumfield TJ, Zhao H, et al. Wood biochar increases nitrogen retention in field settings mainly through abiotic processes. Soil Biology and Biochemistry. 2015;90:232-40.
87. Bailey AC, Kellom M, Poret-Peterson AT, Noonan K, Hartnett HE, Raymond J. Draft Genome Sequence of Massilia sp. Strain BSC265, Isolated from Biological Soil Crust of Moab, Utah. Genome Announcements. 2014;2(6):e01199-14, 2/6/e-14.
88. <Cacciari et al. - 1986 - Ammonium assimilation in an Arthrobacter sp. "fluo.pdf>.
89. Cacciari I, Lippi D, Pietrosanti T, Pietrosanti W. Ammonium assimilation in an Arthrobacter sp. "fluorescens". Archives of Microbiology. 1986;145(2):113-5.
90. Liu Y, Zhang Y, Huang Y, Niu J, Huang J, Peng X, et al. Spatial and temporal conversion of nitrogen using Arthrobacter sp. 24S4-2, a strain obtained from Antarctica. Front Microbiol. 2023;14:1040201.
91. Granja-Travez RS, Persinoti GF, Squina FM, Bugg TDH. Functional genomic analysis of bacterial lignin degraders: diversity in mechanisms of lignin oxidation and metabolism. Appl Microbiol Biotechnol. 2020;104(8):3305-20.
92. Weiland F, Kohlstedt M, Wittmann C. Guiding stars to the field of dreams: Metabolically engineered pathways and microbial platforms for a sustainable lignin-based industry. Metabolic Engineering. 2022;71:13-41.
93. Parke D, D'Argenio DA, Ornston LN. Bacteria Are Not What They Eat: That Is Why They Are So Diverse. Journal of Bacteriology. 2000;182(2):257-63.
94. Buchan A, Neidle EL, Moran MA. Diverse organization of genes of the beta-ketoadipate pathway in members of the marine Roseobacter lineage. Appl Environ Microbiol. 2004;70(3):1658-68.
95. Pérez-Pantoja D, Donoso R, Agulló L, Córdova M, Seeger M, Pieper DH, et al. Genomic analysis of the potential for aromatic compounds biodegradation in Burkholderiales. Environmental Microbiology. 2012;14(5):1091-117.
96. Song J, Sung J, Kim YM, Gerben J Z, Kim E. Roles of the meta- and the ortho-Cleavage Pathways for the Efficient Utilization of Aromatic Hydrocarbons by Sphingomonas yanoikuyae Bl. Korean Journal of Microbiology. 2002;38(4):245-.
97. Aghapour AA, Moussavi G, Yaghmaeian K. Biological degradation of catechol in wastewater using the sequencing continuous-inflow reactor (SCR). J Environ Health Sci Eng. 2013;11:3.
98. <Basha et al. - Recent advances in the Biodegradation of Phenol A.pdf>.

99. Basha KM, Rajendran A, Thangavelu V. Recent advances in the Biodegradation of Phenol: A review. 2010;1:219-34.
100. Baldani JI, Rouws L, Cruz LM, Olivares FL, Schmid M, Hartmann A. The Family Oxalobacteraceae. In: Rosenberg E, DeLong EF, Lory S, Stackebrandt E, Thompson F, editors. The Prokaryotes. Berlin, Heidelberg: Springer Berlin Heidelberg; 2014. p. 919-74.
101. Li X, Gou X, Long D, Ji Z, Hu L, Xu D, et al. Physiological and metabolic analysis of nitrate reduction on poly-gamma-glutamic acid synthesis in Bacillus licheniformis WX-02. Archives of Microbiology. 2014;196(11):791-9.

Figure 1. Non-metric multidimensional scaling (NMDS) of geTMM normalized a) PyOM b) alkane c) Nitrogen and d) urea cycling genes within the microbial communities of burned and unburned soil samples (color) and time since fire (days; shape). Treatment and time since fire effects based on PERMANOVA ($p < 0.05$). Ellipse represents the 95% confidence level.

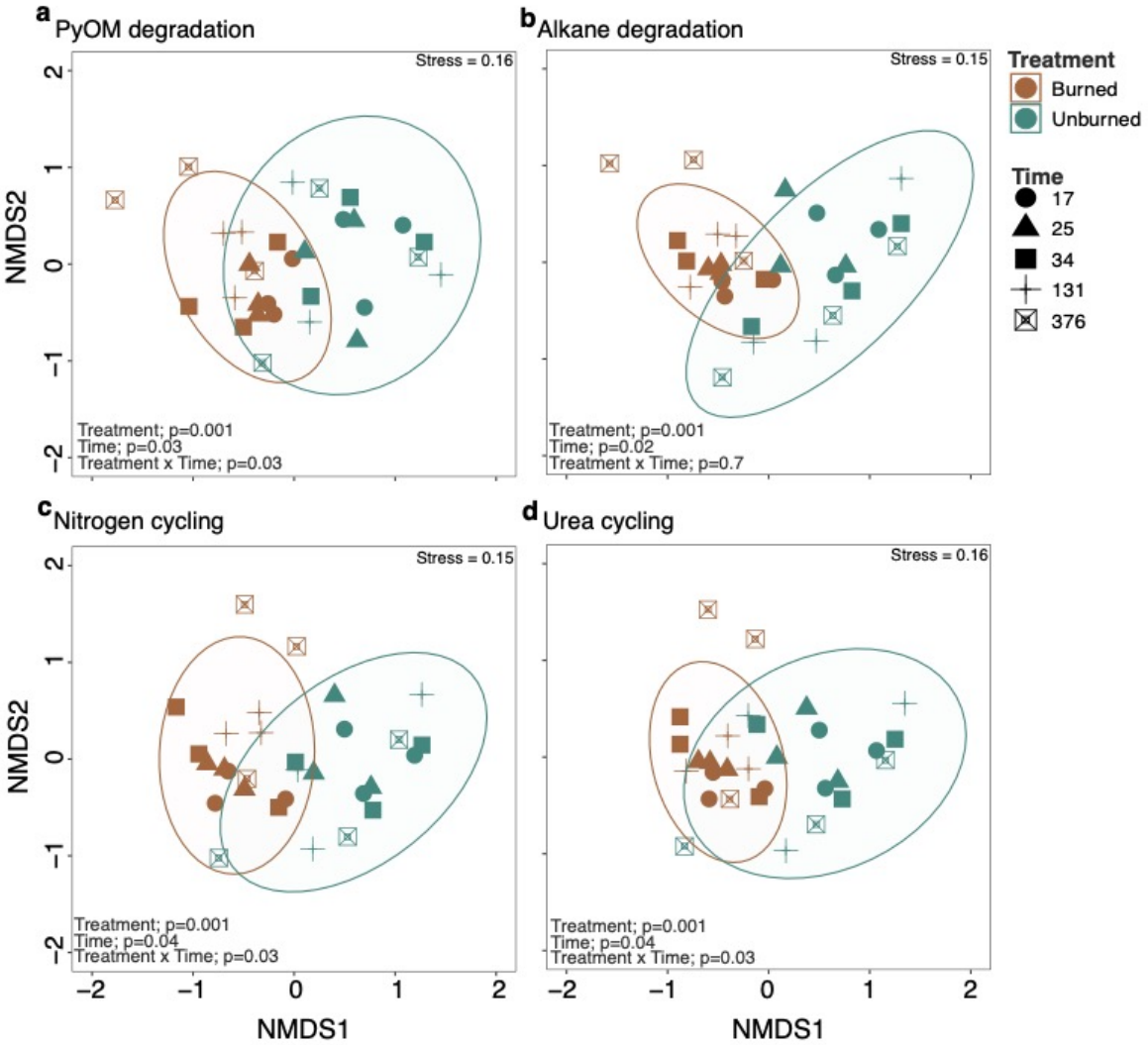

Figure 2. Principal component analysis (PCoA) of the mean and standard error Bray-Curtis community dissimilarity at each timepoint for the unburned and burned a,b) PyOM; c,d) Alkane; e, f) nitrogen and g, h) urea functional potentials. Note that timepoints further apart with nonoverlapping standard error bars indicate a community turnover, whereas overlapping standard error bars represent a lack of compositional turnover, with the first sampling time point at 17 days representing the base level. Thus, the first turnover was initiated at 25 days. There were no significant turnover dates for any gene functional potentials in the unburned plots. The days with significant turnovers in the burned plots are listed in the upper right corners. Significance based on betadisper, which measures the dispersion/variability of the data within groups as a means to measure community turnover.

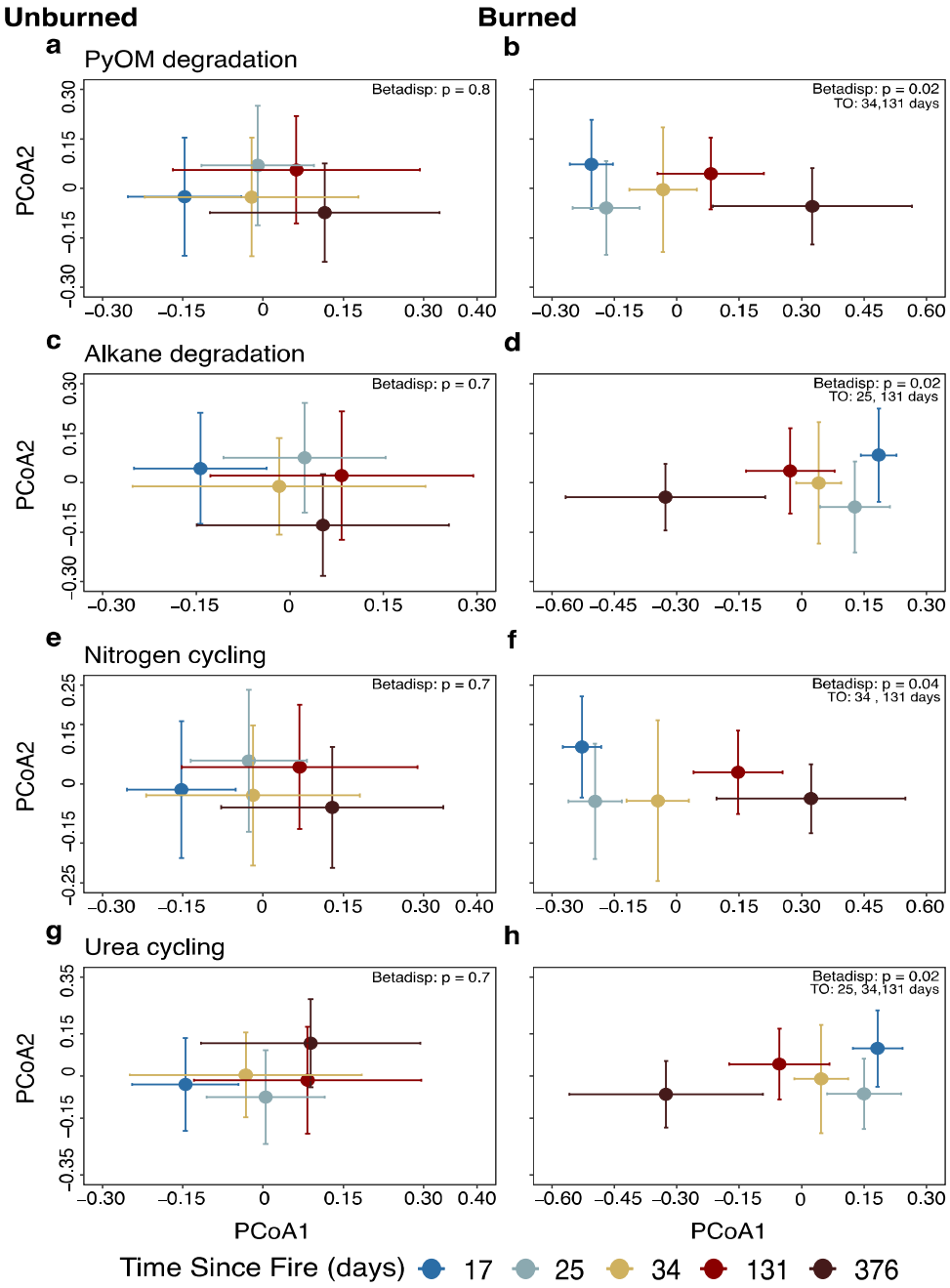

Figure 3. Summed geTMM normalized gene abundance over time for a,b) PyOM and c, d) Alkane degradation in the unburned (left panel) and burned (right panel). Colors are based on the general function for each gene.

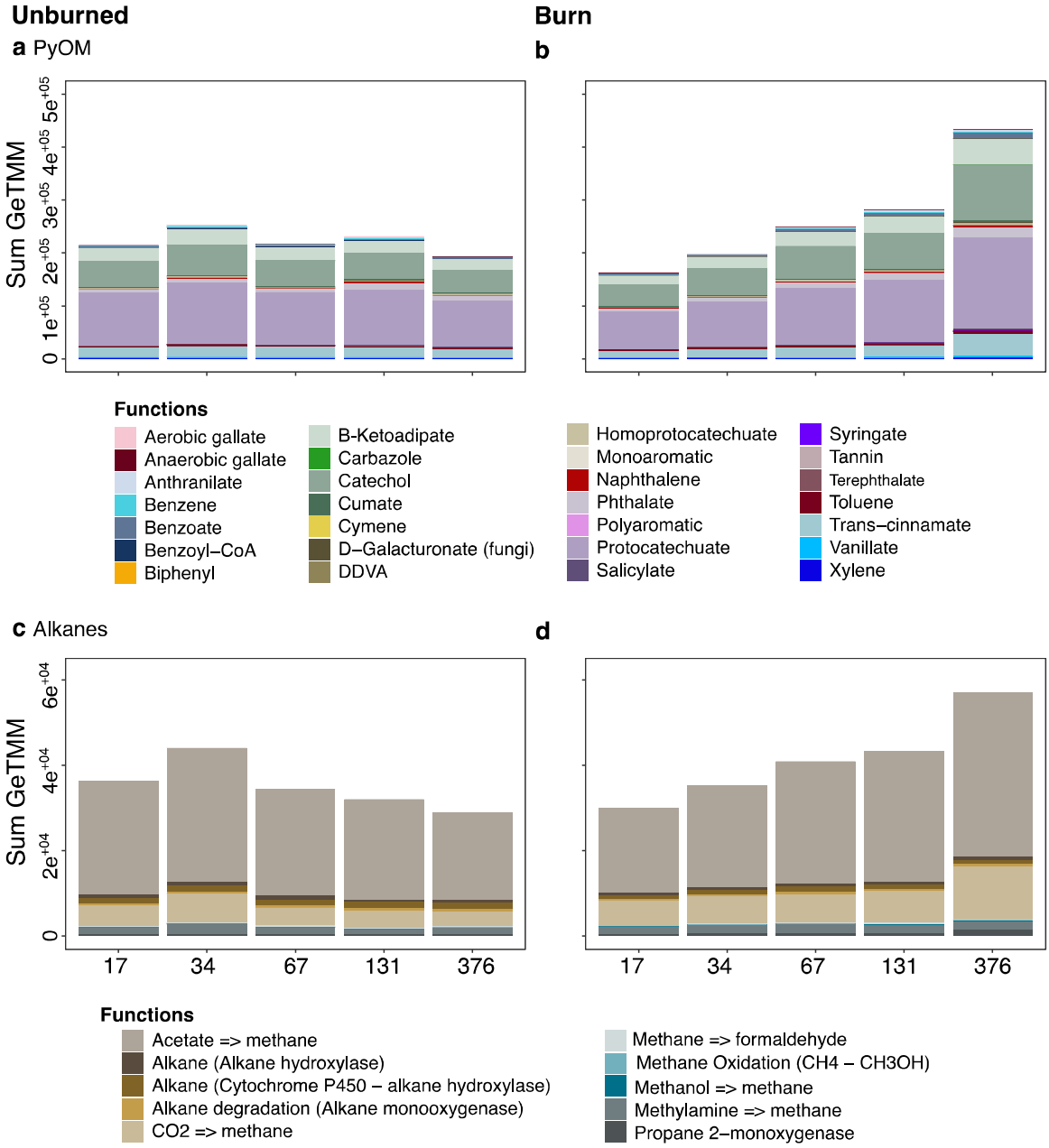

Figure 4. Summed geTMM normalized gene abundance over time for a,b) Nitrogen and c, d) Urea cycling genes in the unburned (left panel) and burned (right panel). Colors are based on the general function for each gene.

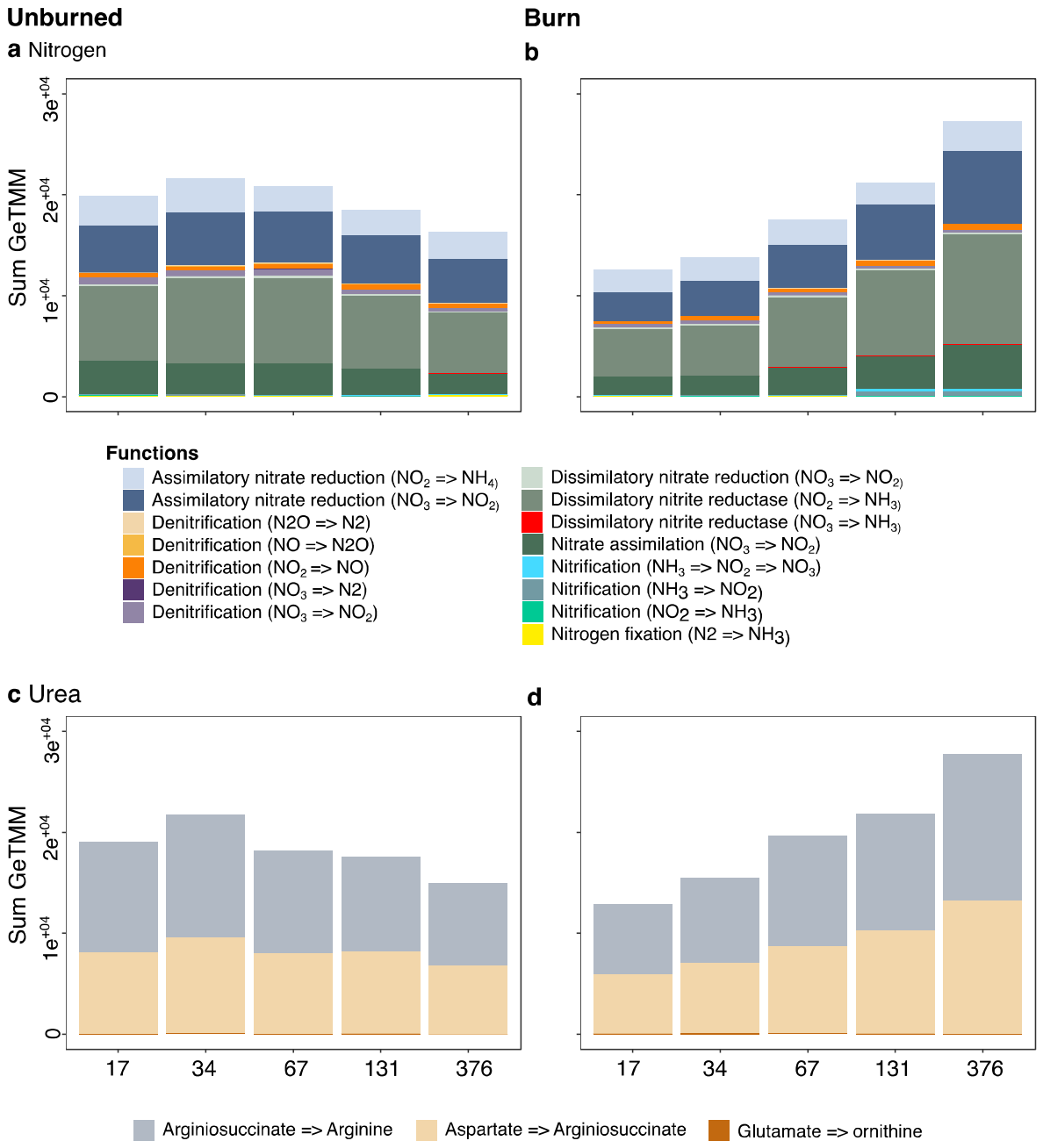

Figure 5. Total number of genes that were differentially abundant in the burned plots (brown) versus the unburned plots (blue green; x axis) per each metabolic pathway, colored by each sampling time point for a) PyOM, b) Alkane, Nitrogen and d) Urea cycling. Significance based on DESeq2 Wald test (adjusted P value < 0.05 and absolute log2 fold-change >0).

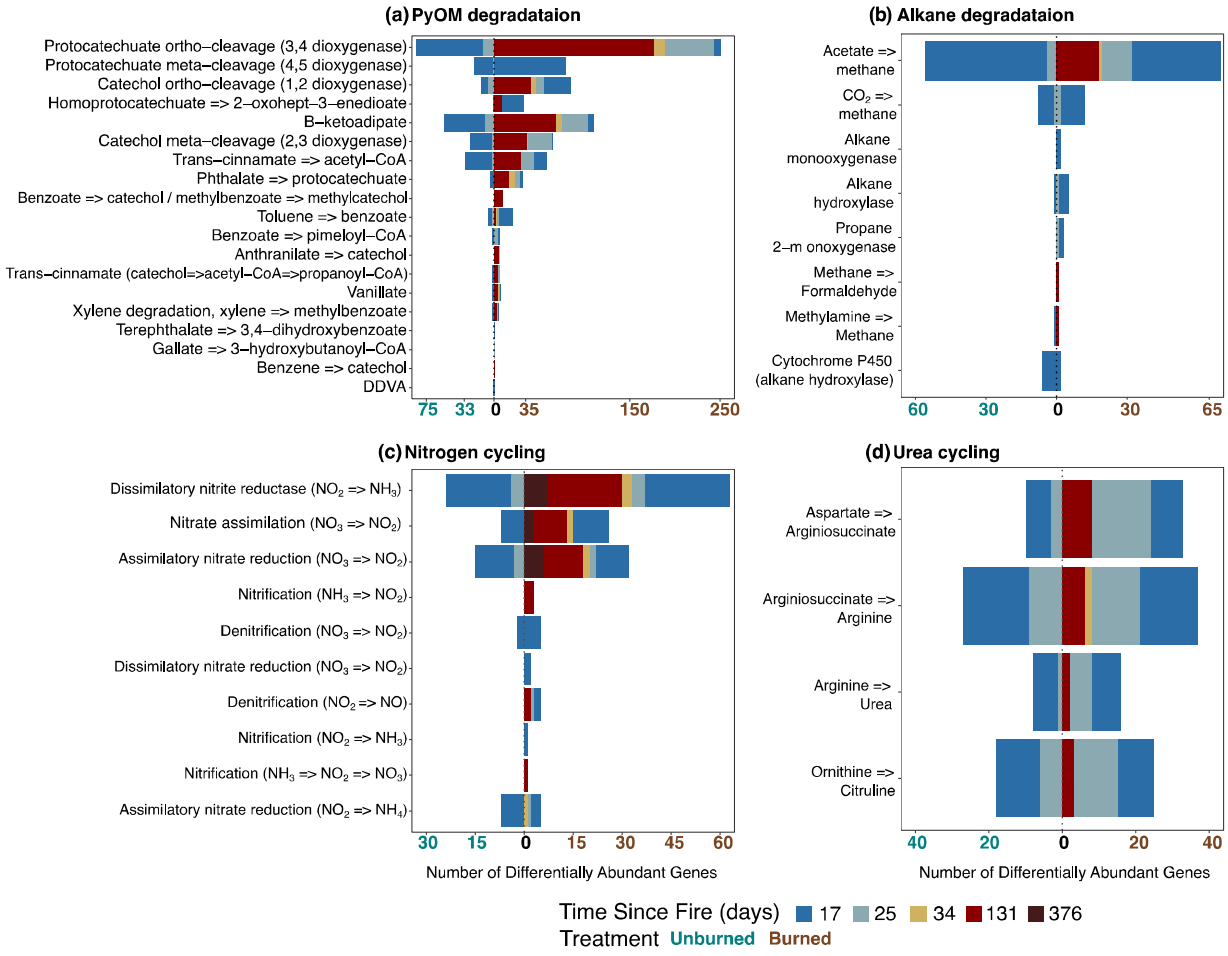

Figure 6. The catechol and protocatechuate degradation pathways with arrows indicating genes that were differentially expressed in the burned treatment at each time point (17, 25, 34, 131 and 376 days post-fire; Wald's test in DESeq2; $p<0.05$). Line type represents catechol (solid) and protocatechuate (dashed) cycling pathways and gray solid lines represent pathways that were not expressed during post-fire year one. Numbers in parentheses represent the mean log2fold change (DESeq2) for each represented gene and are colored by the timepoint in which that gene was significantly abundantly represented.

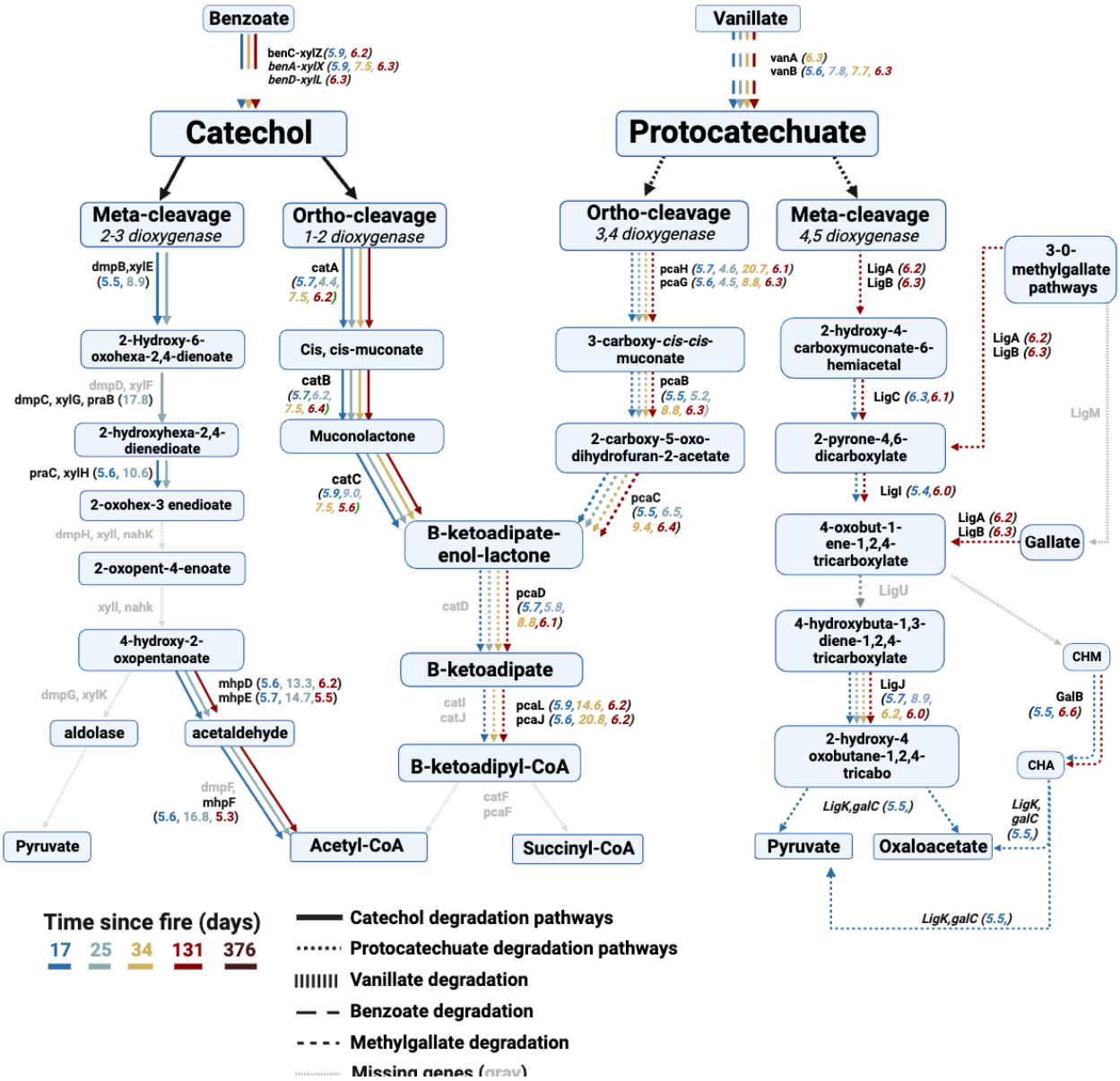

Figure 7. The nitrogen cycle with arrows indicating genes that were differentially represented in the burned treatment at each time point (17, 25, 34, 131, and 376 days post-fire; Wald's test in DESeq2; $p<0.05$). Line type represents the different nitrogen cycling pathways, colored by timepoint and gray solid lines represent pathways that were not expressed during post-fire year one. Numbers in parentheses represent the mean log2fold change (DESeq2) for each represented gene and are colored by the timepoint in which that gene was significantly abundantly represented.

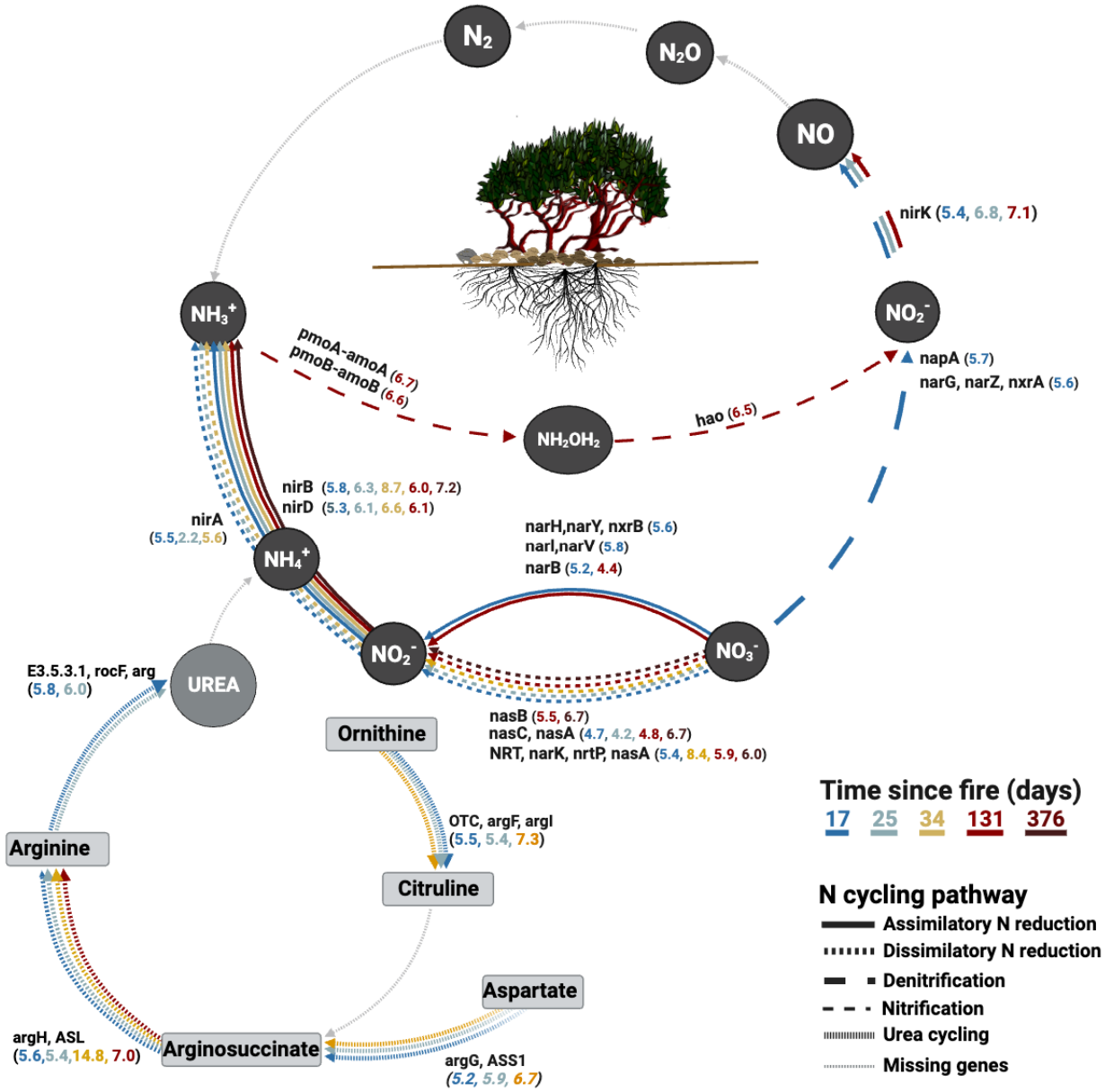
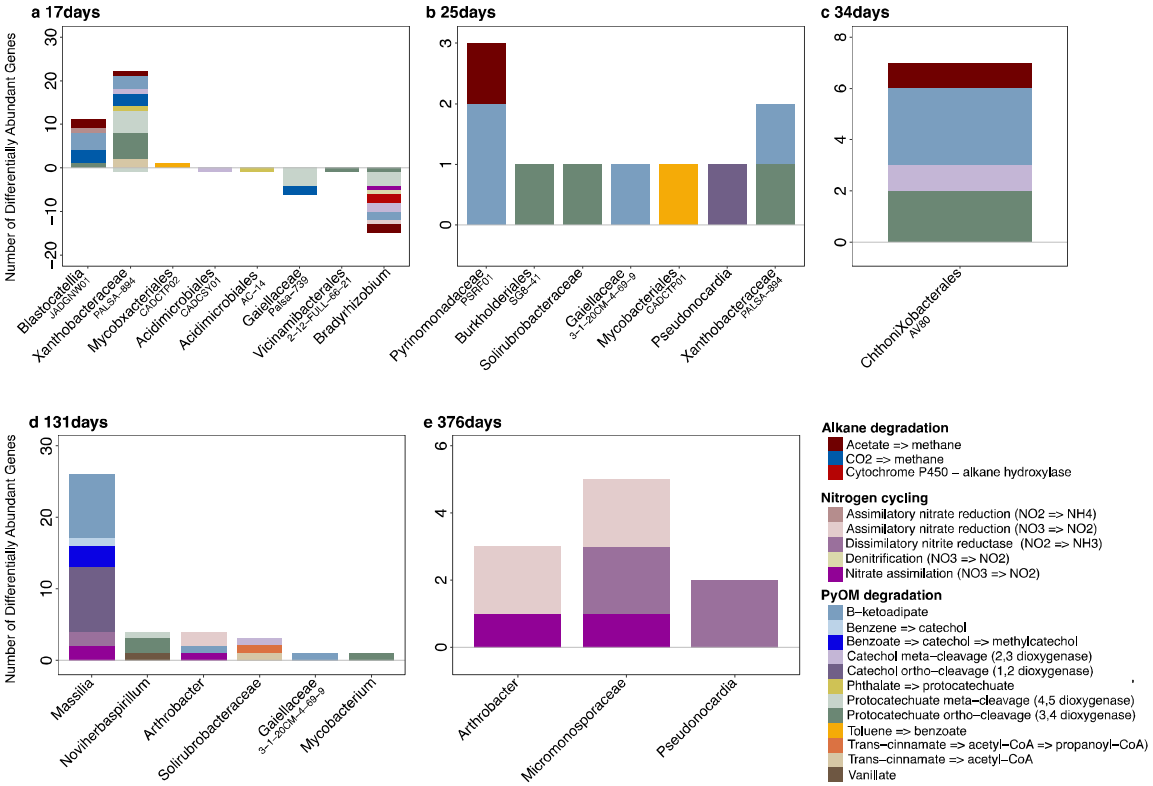
Figure 8. Taxonomic annotation for the most dominant, differentially abundant PyOM, nitrogen and urea genes based on DESeq analysis (adjusted P value < 0.05 and absolute log2 fold-change >0). Taxonomy based on blasting contigs against the Metagenome Assembled Genomes (MAGs) represented in the x-axis.